Chapter 11

Partitioning of Nonionic Organic Compounds Between Well-Defined Surfaces and Air or Water

Environmental Organic Chemistry, Third Edition. René P. Schwarzenbach, Philip M. Gschwend, and Dieter M. Imboden.
Copyright © 2017 John Wiley & Sons, Inc. Published 2017 by John Wiley & Sons, Inc.
Companion website: www.wiley.com/go/Schwarzenbach/EnvironmentalOrganChem3e

11.1 Introduction

In the previous chapters on equilibrium partitioning, our discussions focused on molecules penetrating *into* bulk phases, such as benzene dissolving in water, which is referred to as *absorption* into a phase. We assumed that (1) the presence of the compound of interest did not influence the properties of the phases considered and (2) the partition constant was independent of solute concentration, with the case of liquid organic mixtures (Section 10.4) being an exception. In this chapter, we focus on the partitioning of organic compounds *to* solid and liquid surfaces, a process termed *adsorption*. Such two-dimensional surfaces only have a limited number of sites available for adsorption. Hence, the partition "constant" may change with increasing compound (*sorbate*) concentration in the bulk phase due to the corresponding increasing surface coverage.

In this chapter, we are primarily interested in understanding and quantifying the molecular interactions governing adsorption to well-defined surfaces. Therefore, we consider only cases in which compound concentrations are small enough so we can assume a concentration-independent partitioning (adsorption) constant, as we did for absorption processes. We also limit the discussion to neutral compounds that do not interact specifically with charged surface species via complexation or electrostatic interactions. Ionic interactions, which are particularly important in aquatic systems, are addressed in Chapter 14. The main focus of this chapter is on adsorption of such nonionic compounds from the gas phase (i.e., air) to inorganic surfaces including water and ice surfaces, mineral surfaces, and salt surfaces. We also briefly address some organic surfaces for comparison; partitioning to organic surfaces, in particular to carbonaceous materials, is discussed in Chapter 13.

11.2 Adsorption from Air to Well-Defined Surfaces

In the environmental assessment of nonionic organic chemicals, transfer processes between air and natural surfaces are frequently neglected. Absorption of such chemicals from air into bulk phases such as water or organic phases is assumed to be the dominant partitioning process. However, adsorption, particularly to inorganic surfaces, may be more important than absorption in situations such as transfer from air to snow or ice surfaces; to the surfaces of small water droplets (< 10 μm) in fog; to inorganic aerosols as encountered above the sea (i.e., salts), above deserts (i.e., mineral dust), or in urban areas (e.g., carbonaceous materials); and, last but not least, to abundant soil minerals such as quartz and clays, particularly at low humidity. Knowledge of the adsorption behavior of organic chemicals from air onto surfaces of solids or liquids is also important for indoor and outdoor air quality assessments and the design of engineered systems including air purification systems (e.g., filters). Unfortunately, to date, rather few studies have systematically investigated the exchange of organic chemicals between the gas phase and environmentally important inorganic surfaces. Nevertheless, since from a molecular interaction point of view, adsorption from the air to a *surface* of a condensed phase (Fig. 11.1) is somewhat easier to treat than absorption processes involving bulk phases where cavity formation has to be

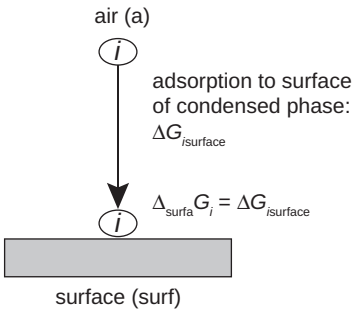

Figure 11.1 Adsorption of a compound *i* from air (assuming an ideal gas phase) to a surface of a condensed phase.

taken into account (see Fig. 7.1), some important general insights into this process are possible with the limited experimental data available.

Characteristics of Mineral Surfaces

Among the inorganic surfaces, mineral surfaces are the most significant for adsorption processes involving gaseous organic compounds in the environment. Many common minerals expose a surface to the exterior that consists of hydroxyl groups protruding into the medium from a "checker board" plane of electron-deficient metals (e.g., Si, Al, Fe) and electron-rich ligands (e.g., hydroxyl, carbonate) (Fig. 11.2*a*). Like water molecules, these surface groups typically include a combination of hydrogen donors (e.g., –OH, –C(=O)OH) and acceptors (–OH, –C(=O)OH, and –O–). Therefore, such bipolar surfaces interact with molecules adjacent to the mineral surface via vdW, H-donor, and H-acceptor interactions. We can use data of pure liquid:silica solid attractions (Fowkes, 1964) to understand the relative contributions of such molecule:surface interactions (Fig. 11.2*b*). While all sorbates are attracted to all surfaces by vdW forces, stronger attractions per unit surface area of silica are observed as complementary functional groups are included on the surface and the sorbate that are capable of H-bonding (note that the free energies of adsorption, $\Delta_{\text{surfa}} G_i$, are in mJ m^{-2}). This surface attraction energy is very strong for an H-donor and H-acceptor sorbate like water (−460 mJ m^{-2}), as compared to other small nonionic organic compounds (Fig. 11.2*b*). Thus, such surfaces strongly prefer to bind water, and the overall energy change resulting from adsorption of organic chemicals directly to water-wet solids would have to include the high "cost" of desorption of water from the same surface.

In the environment, minerals are almost always exposed to water vapor, and one may reasonably expect these natural polar surfaces are water-wet. The extent of the water coverage, however, can vary. The amount of water at a mineral surface is proportional to the activity of water in the atmosphere (i.e., the ratio of water's partial pressure to its saturation pressure at the particular temperature); the saturation vapor pressure of water at ambient temperatures corresponds to about 1 mol of water per m^3 of air. Commonly, such water activity is quantified in terms of "relative humidity" (RH) where 100% RH implies the air is equilibrated with pure water liquid, thus the activity of the water in the atmosphere is equal to 1. Therefore, the extent of water coverage at a surface can be related to RH (Fig. 11.3*a*). The first monolayer of water (a one water molecule-thick layer everywhere) occurs at RH conditions much less than 100%. For example, many pure mineral oxides exhibit monolayer coverage at about 30% RH (Goss and Schwarzenbach, 1999a; Goss, 2004). Compositionally heterogeneous soils have been reported to have monolayer quantities of water at less than 20% RH (Chiou and Shoup, 1985). At greater RH, this layer of water on which other sorbates adsorb grows thicker and thicker (see Fig. 11.3*b*). For example, Chiou and Shoup (1985) observed that adsorbed water on a soil equaled about three times monolayer coverage at 80% RH.

As the water coverage at a mineral surface changes with RH, so does the affinity for organic compounds adsorbing from the gas phase. At lower water coverage, vdW and H-bonding interactions directly with the mineral surface drive attraction. Once water coverage at a mineral surface reaches about five to six monolayers, the

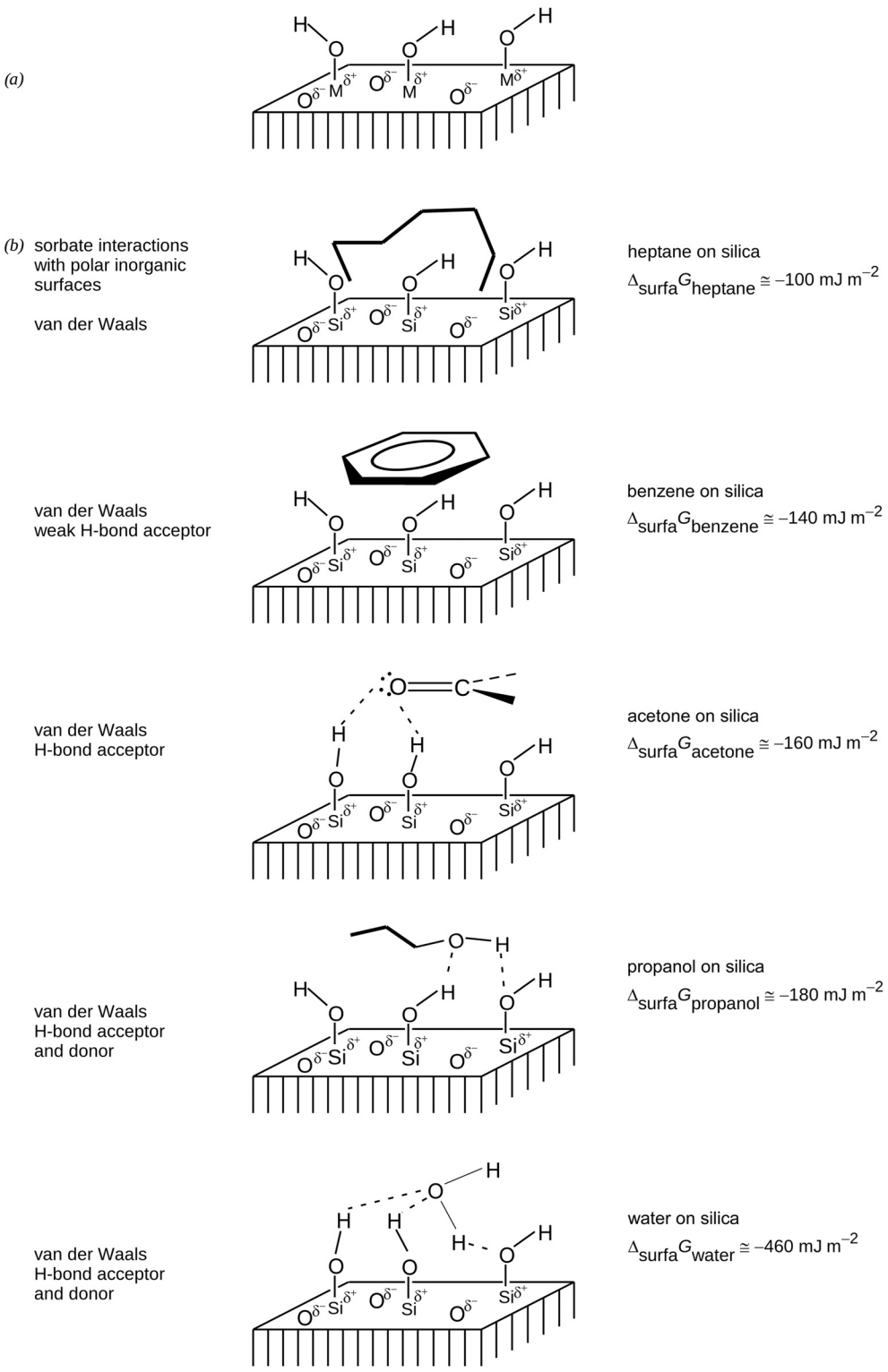

Figure 11.2 (*a*) A schematic view of a mineral surface exhibiting loci of partial positive charges where metal atoms occur ($M^{\delta+}$) and partial negative charges where linking anions occur ($O^{\delta-}$) and hydroxyls extending to the exterior. (*b*) Interactions of organic chemicals wetting silica surfaces and estimates of the $\Delta_{surfa}G_i$ values derived from surface tension data (Fowkes, 1964).

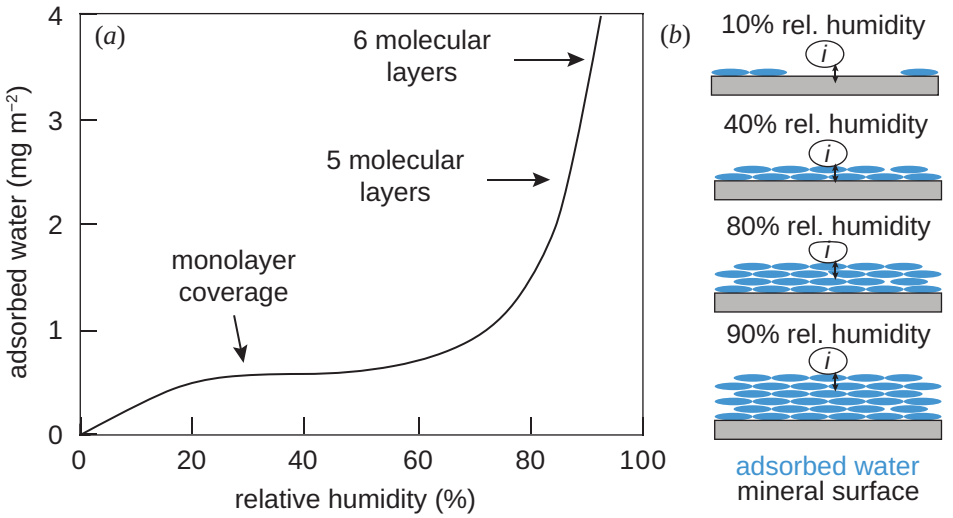

Figure 11.3 (*a*) Typical increase of adsorbed water on a mineral oxide surface as function of relative humidity. (*b*) Illustration of adsorption of neutral organic compounds to polar mineral surface with varying water surface coverage (related to RH).

surface properties of the water film, particularly those describing vdW interactions, resemble those of pure water. As such, much weaker molecular interactions, as compared to a "dryer" mineral surface (at low RH), drive attraction of organic pollutants. This decrease in attraction is illustrated by Fig. 11.4, which shows the adsorption of 1,3-dichlorobenzene to a soil at different RH. At 0% RH, adsorption is strongest and decreases with increasing RH; at 90% RH, adsorption is minimal. In conclusion, as we continue our discussion of adsorption, we need to remember that *partially water-wet mineral surfaces, not completely dry surfaces, must be considered as adsorbents of organic chemicals from air and that the amount of water coverage is important.*

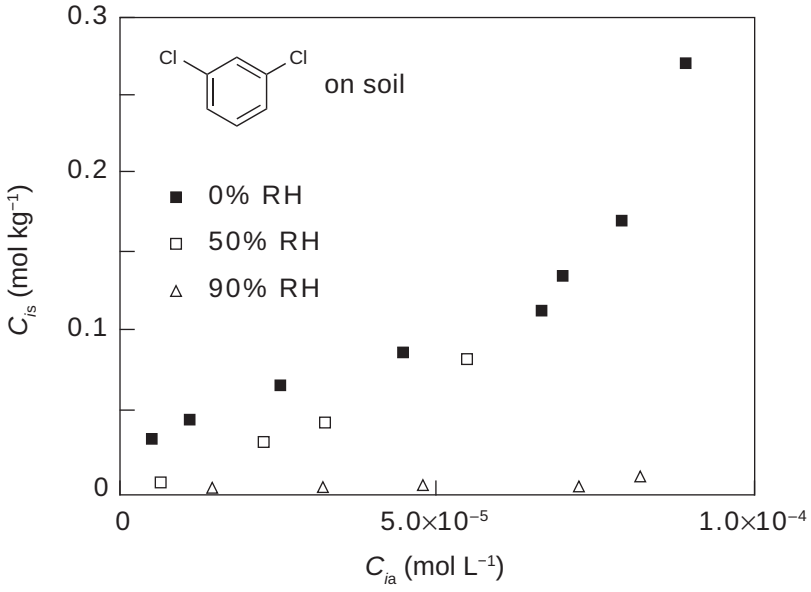

Figure 11.4 Adsorption of 1,3-dichlorobenzene on Woodburn soil at 20°C at different relative humidities. Data from Chiou and Shoup (1985).

Surface–Air Partition Constants: Definition and Temperature Dependence

Since adsorption to a surface is proportional to the available surface area of the condensed phase, we define the equilibrium partition coefficient, $K_{i\text{surfa}}$, as the concentration of the compound on the surface per *unit surface area* of the condensed phase divided by the concentration in air:

$$K_{i\text{surfa}}(\text{e.g., m}) = \frac{C_{i\text{surf}}(\text{e.g., mol m}^{-2}\text{ surf})}{C_{ia}(\text{e.g., mol m}_a^{-3})} \tag{11-1}$$

Hence, $K_{i\text{surfa}}$ is expressed, for example, in $m_a^3\ m^{-2}$ surface which we denote in Eq. 11-1 simply as m. If the surface area is not known, the partition constant is normalized to the mass of the solid (subscript s):

$$K_{isa}(\text{e.g., L}_a\text{ kg}^{-1}\text{ solid}) = \frac{C_{is}(\text{e.g., mol kg}^{-1}\text{ solid})}{C_{ia}(\text{e.g., mol L}_a^{-1})} \tag{11-2}$$

As the adsorption process, however, is a surface process, the normalized K_{isa} derived for a particular inorganic solid is not directly applicable to the same material from another source. We assume that $K_{i\text{surfa}}$ or K_{isa} is not dependent on the concentration of the compound at the surface; that is, we assume that the sorbing compound molecules, *i*, do not "feel each other" at the solid surface as the surface is far from saturated. All sites at the surface are assumed to be equally interactive with respect to intermolecular interactions, leading to a "linear adsorption isotherm" (see Chapter 12).

With respect to the effect of temperature on $K_{i\text{surfa}}$, as for all other partition processes discussed so far, we need to know the enthalpy of the phase transfer, in this case $\Delta_{\text{surfa}}H_i$. As stated in Chapter 4 (Section 4.2), the molar volume of gases is temperature dependent, and so if the partition constant is expressed in molar concentrations, $\Delta_{\text{surfa}}H_i$ has to be replaced by $\Delta_{\text{surfa}}H_i + RT_{\text{av}}$, where T_{av} is the average temperature (in K) of the temperature range considered (Atkinson and Curthoys, 1978). However, because RT_{av} is only about 2.5 kJ mol^{-1}, we neglect this term. Hence, we write:

$$\ln K_{i\text{surfa}}(T) = -\frac{\Delta_{\text{surfa}}H_i}{R}\frac{1}{T} + \text{const} \tag{11-3}$$

Similar to the prediction of enthalpies of vaporization from vapor pressure data (Eq. 8-14), Goss and Schwarzenbach (1999b) derived an empirical relationship to estimate $\Delta_{\text{surfa}}H_i$ from $K_{i\text{surfa}}$ at 15°C (288K):

$$\Delta_{\text{surfa}}H_i(\text{kJ mol}^{-1}) = -9.83 \log K_{i\text{surfa}}(\text{m}) - 90.5 \tag{11-4}$$

As verified by Arp et al. (2006a), Eq. 11-4 predicts $\Delta_{\text{surfa}}H_i$ with a standard error of less than ± 15 kJ mol^{-1}, which, for most practical applications, is sufficient. Hence,

assuming $\Delta_{surfa}H_i$ is constant over the ambient temperature range, we can estimate the surface–air partition constant at any other temperature by:

$$K_{isurfa}(T) = K_{isurfa}(288\text{K})\, e^{-\frac{\Delta_{surfa}H_i(288\text{K})}{R}\left(\frac{1}{T}-\frac{1}{288}\right)} \quad (11\text{-}5)$$

sp-LFER Modeling Approach to Estimate Surface–Air Partitioning

The traditional and still most widely used approach to estimate surface–air partition constants is to apply simple single-parameter LFERs (sp-LFERs) relating K_{isurfa} to the liquid vapor pressure, p^*_{iL}, of the compound:

$$\log K_{isurfa}(T)(\text{m}) = -a\, \log p^*_{iL}(T)(\text{Pa}) + b \quad (11\text{-}6)$$

Similar to the sp-LFERs applied earlier to estimate bulk phase–air and bulk phase–water partition constants or coefficients using, for example, octanol–air or octanol–water partition constants (see Chapters 7 and 10), the slope, a, and the intercept, b, in Eq. 11-6 are determined by a linear regression analysis of a set of compounds with known K_{isurfa} values. We use a minus sign for the term $\log p^*_{iL}$ since we use the surface–air and not the air–surface partition constant. Figure 11.5 shows the application of Eq. 11-6 to adsorption from air to a quartz surface at 90% RH; good relations are restricted to structurally related compounds, particularly for mono- and bipolar compounds adsorbing to this polar surface. Furthermore, as previously discussed (Figs. 11.3 and 11.4), even when considering the same surface, the system's RH may have a large impact on K_{isurfa}. Thus, for a given surface, one has to derive not only different sp-LFERs for different groups of compounds but also for different RHs. Since a

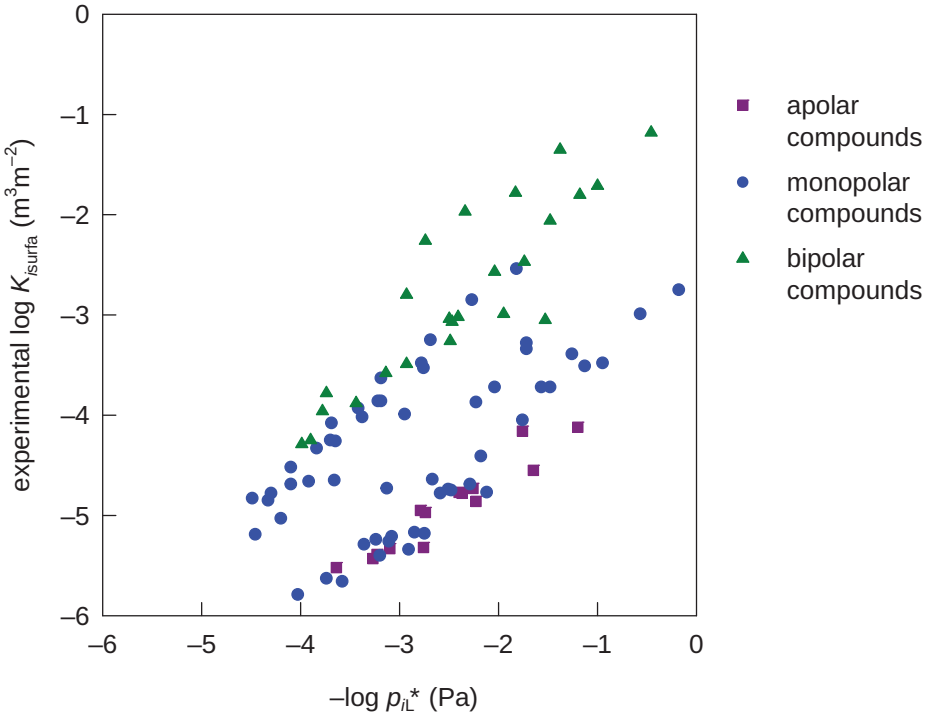

Figure 11.5 Experimental K_{isurfa} values for different apolar, monopolar, and bipolar compounds on a quartz surface at 90% RH versus liquid vapor pressure, p^*_{iL}, of the compound. Data from Arp et al. (2006a).

model that incorporates both compound and surface variability in one equation would be highly advantageous, we now turn to pp-LFERs.

pp-LFER Modeling Approach to Estimate Surface–Air Partitioning

As depicted in Fig. 11.1, adsorption to a surface, including water-wet mineral surfaces, does not involve any cavity formation. As a consequence, we do not need to consider such a contribution when describing the free energy of surface–air partitioning as we have done for bulk phase–air partitioning (see Chapter 7, Fig. 7.1). Therefore, the surface–air partition constant can be simply related to the free energy of transfer from the gas phase to the surface:

$$\log K_{i\text{surfa}} = -\Delta_{\text{surfa}} G_i / 2.303RT + \text{constant} \qquad (11\text{-}7)$$

The constant in Eq. 11-7 depends on the units of $K_{i\text{surfa}}$, and the chosen air and surface standard states. As proposed by Goss (2004), when only considering interactions of the compound with the surface (vdW and H-bonding), using the units defined in Eq. 11-1, and defining the surface standard state as proposed by de Boer (1968), Eq. 11-7 can be written as:

$$\log K_{i\text{surfa}}(\text{m}) = -\left(\Delta^{\text{vdW}}_{i\text{surf}} G_i + \Delta^{\text{H}}_{i\text{surf}} G_i\right) / 2.302RT - 8.47 \qquad (11\text{-}8)$$

or as expressed by introducing corresponding vdW and H-bonding pp-LFER terms:

$$\log K_{i\text{surfa}}(\text{m}) = a_1(\text{vdW}_i)(\text{vdW}_{\text{surf}}) + a_2(\text{HD}_i)(\text{HA}_{\text{surf}}) + a_3(\text{HA}_i)(\text{HD}_{\text{surf}}) - 8.47 \qquad (11\text{-}9)$$

In contrast to pp-LFERs used for bulk phase partitioning introduced in Chapter 7 (Eq. 7-12) then used throughout Chapters 8 to 10, we only need three terms to describe adsorption from air to surfaces, and we explicitly express the corresponding surface parameters. The coefficients a_1, a_2, and a_3 are scaling factors that depend on the specific parameters used for the description of the vdW and H-bonding terms and, of course, on temperature. In bulk partitioning, the system descriptors (i.e., *v, e, l, s, a, b)* include scaling and characterization of the bulk phases involved.

Using the same solute descriptors as for bulk phase partitioning (L_i, A_i, and B_i), Eq. 11-9 can be expressed as:

$$\log K_{i\text{surfa}}(\text{m}) = a_1(\text{vdW}_{\text{surf}})L_i + a_2(\text{HA}_{\text{surf}})A_i + a_3(\text{HD}_{\text{surf}})B_i - 8.47 \qquad (11\text{-}10)$$

We now need to define the parameters for vdW and H-bonding interactions (vdW_{surf}, HA_{surf}, and HD_{surf}) for a surface in order to solve Eq. 11-10 and apply it to specific surfaces.

Parameters for vdW and H-Bonding Interactions for Surfaces. The first parameter in Eq. 11-10, the vdW surface parameter vdW_{surf}, may be expressed by the square root of the vdW component of the surface free energy, $\sqrt{\gamma^{\text{vdW}}_{\text{surf}}}$, which can be determined independently (Goss, 2004). For water, $\sqrt{\gamma^{\text{vdW}}_{\text{surf}}}$ is 4.7 $(\text{mJ m}^{-2})^{0.5}$; values for various

Table 11.1 Van der Waals (vdW_{surf}), H-Acceptor (Electron Donor) (HA_{surf}), and H-Donor (Electron Acceptor) (HD_{surf}) Values for Some Condensed Phases at 15°C (or as stated)[a]

Surface	Relative Humidity (RH, %)[b]	vdW_{surf}[c] $(mJ\ m^{-2})^{0.5}$	HA_{surf}[d]	HD_{surf}[d]
Inorganic Surfaces				
Water	100	4.7	1.0	1.0
Water (0°C)	100	4.7	n.a.	n.a.
Ice (0°C)	100	5.4	n.a.	n.a.
Quartz (SiO_2)	45	6.8	0.89	1.06
	90	5.3	0.88	0.85
Ca-kaolinite	30	7.0	n.a.	1.12
	90	4.7	n.a.	0.75
Hematite (Fe_2O_3)	30	6.5	n.a.	0.92
	90	4.8	n.a.	0.76
Limestone ($CaCO_3$)	40	5.4	1.20	0.96
	90	4.9	1.01	0.91
Corundum (Al_2O_3)	40	5.4	1.13	1.00
	90	4.8	1.05	0.89
KNO_3	35	7.1	0.99	0.75
	60	6.8	1.00	0.70
$(NH_4)_2SO_4$	35	6.6	1.08	0.73
	70	6.3	1.34	0.53
NH_4Cl	35	6.8	1.19	0.75
	60	6.3	1.21	0.69
NaCl	35	6.2	1.11	0.79
	60	6.0	1.06	0.77
Organic Surfaces				
Paraffin wax ($H–(CH_2)_n–H$)	n.r.	5.0	0	0
Teflon ($F–(CF_2)_n–F$)	n.r.	4.2	0	0
Nylon 6,6	n.a	6.0		
Activated carbon	n.r.	~11		
Graphite	n.a.	10.7–11.5		

[a] Data from Goss (1997), Goss and Schwarzenbach (1999a and 2002), and Goss et al. (2003).
[b] n.r. = not relevant, n.a. = not available. [c] Square root of the van der Waals component of the surface free energy. [d] Relative to the H-acceptor and H-donor properties of water.

other surfaces at different RH are shown in Table 11.1. Values for $\sqrt{\gamma_{surf}^{vdW}}$ for the mineral surfaces, salts, and organic surfaces vary significantly from about 4 (Teflon) to almost 12 (graphite).

An interesting observation can be made when comparing the vdW_{surf} value of the bulk water surface with those of a series of representative mineral surfaces (i.e., quartz, kaolinite, hematite, limestone, corundum). As evident in Fig. 11.6*a*, in all cases, vdW_{surf} decreases significantly with increasing relative humidity (RH) and approaches

the bulk water surface value when approaching water vapor saturation. As discussed earlier, most organic molecules cannot compete well with water for the sorption sites at mineral surfaces. In the presence of water, organic molecules can only adsorb on top of the adsorbed water film (as pictured in Fig. 11.3*b*). With increasing numbers of water layers, the vdW interactions at the surface of the adsorbed water films become more and more independent of the surface type that is underneath the water molecules. Thus, at 90% RH which corresponds to an average of about 5 to 9 molecular layers of adsorbed water (Fig. 11.3*a*), an apolar compound cannot tell the difference between a quartz (SiO_2) and a corrundum (Al_2O_3) surface, while at 20% RH the differences are significant.

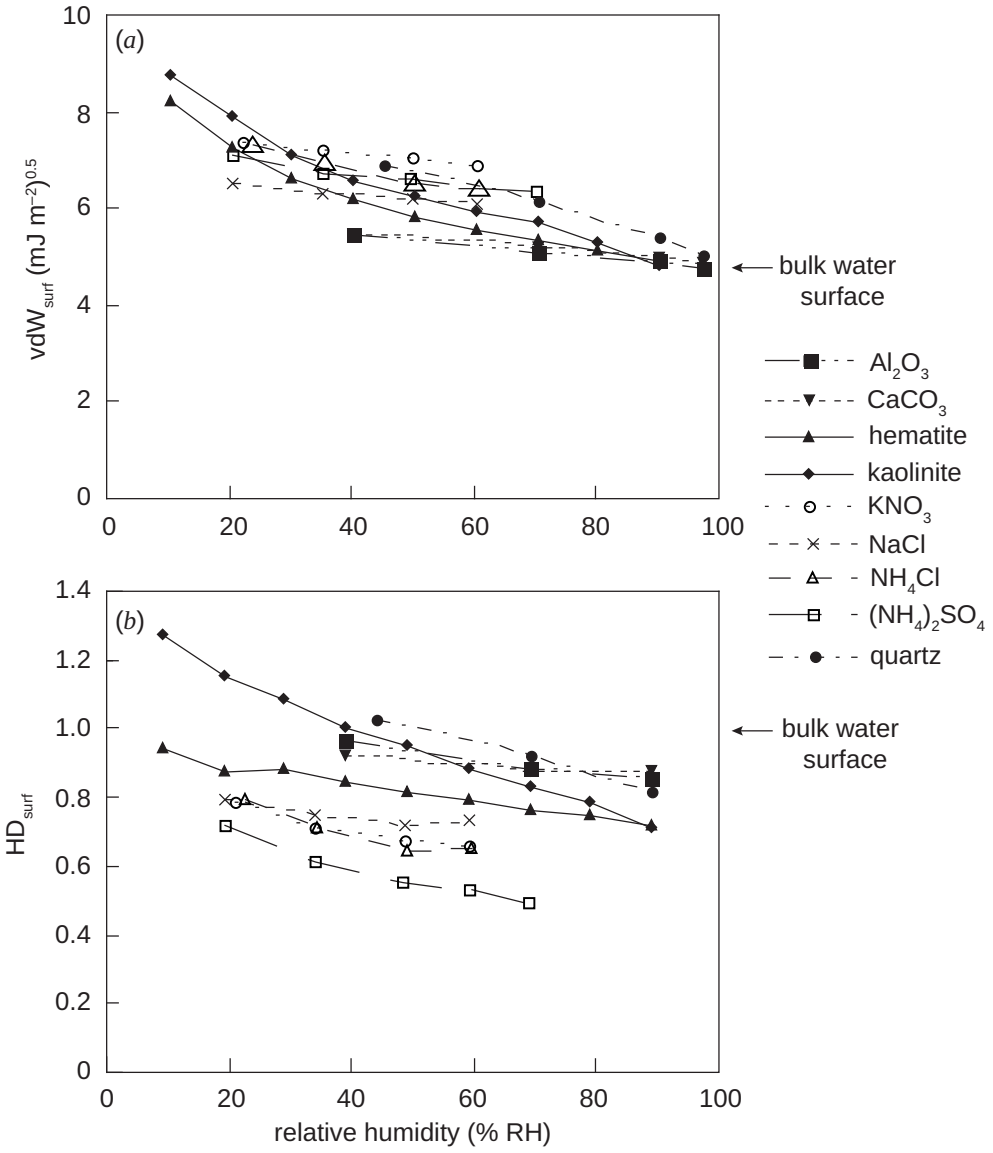

Figure 11.6 (*a*) van der Waals parameter vdW_{surf} and (*b*) H-donor parameters HD_{surf} of various surfaces as a function of relative humidity (RH) at 15 to 20°C. The corresponding values for a bulk water surface are indicated. Data from Goss and Schwarzenbach (1999*a* and 2002); values between 30 and 90% RH are estimated from linear interpolation.

The H-bonding parameters in Eq. 11-10 are not independently measured, but HA_{surf} and HD_{surf} are rather determined according to a scale with water set equal to 1.0 and alkanes set to 0.0 (Goss, 2004). Values for other surfaces, therefore, are relative to a water surface (Table 11.1). For mineral surfaces, the HD_{surf} values decrease with increasing RH and become somewhat more similar among the various surfaces (Fig. 11.6*b*). However, in contrast to the vdW parameter, the values of HD_{surf} at 90% RH (0.65-0.91) are smaller than that of the bulk water surface (1.0). HA_{surf} values for the same surfaces at 90% are often quite similar to the water surface (Table 11.1). These deviations from a water surface may be due to the orientation of the water molecules caused by the nearby solid surface, but a definitive explanation is still missing. Between 90 and 100% RH, when the thickness of the adsorbed water layer rapidly grows, one can expect that these deviations disappear.

Salt surfaces are particularly important when considering partitioning to aerosols in the marine environment. Compared to mineral surfaces, the salt surface parameters exhibit a considerably weaker dependence on RH (Figs. 11.6*a* and *b* and Table 11.1); this weaker dependence is because all four salts considered are hygroscopic and, therefore, adsorb water in significant amounts at low RH. However, the type of underlying salt still has a strong influence on the surface water layer because one can assume that this layer represents a saturated solution of the salt. It is not surprising then that the vdW, the HA_{surf} and the HD_{surf} values of the different salts do not become similar at high RH and that they do not match the values of the pure bulk water surface. Values above 60 or 70% RH are not currently available, but one can assume that they do not change at higher humidity (Goss and Schwarzenbach, 1999a). Finally, for *organic hydrophobic surfaces* (e.g., paraffin wax, polyethylene, polyvinylchloride, polystyrene, Teflon) to which water molecules only weakly adsorb, the effect of humidity can most likely be neglected for all the surface parameters.

As a final note on the surface parameters provided in Table 11.1, we should say that, in general, solid surfaces exhibit chemical and morphological heterogeneities. In this case, different surface sites would have to be described by different surface parameter values. However, on hydrophilic surfaces, the adsorbed water film that is always found at ambient conditions levels out these heterogeneities. Hence, the minerals and salt surfaces in Table 11.1 can be characterized by single values, just like homogenous surfaces.

Applying pp-LFERs to Various Surfaces at Different Relative Humidity. We have now defined the parameters for vdW and H-bonding interactions and can solve Eq. 11-10 using a reference surface and organic sorbents with known solute descriptors (L_i, A_i, and B_i). Roth et al. (2002) used a water surface as a reference, deriving the pp-LFER for adsorption from air to the water surface at 15°C:

$$\log K_{iw\text{surfa}}(288\text{K})(\text{m}) = 0.635L_i + 3.60A_i + 5.11B_i - 8.47 \qquad (11\text{-}11)$$
$$(\text{number of chemicals} = 60; r^2 = 0.932)$$

The fitted Eq. 11-11 for adsorption on a water surface provides the scaling factors a_1, a_2, and a_3 introduced in Eq. 11-10. As these fitted coefficients depend only on

temperature and the scales used to describe the interactions, they can be applied to any surface at 15°C. Thus, for any surface:

$$\log K_{i\text{surfa}}(288\text{K})(\text{m}) = 0.135\sqrt{\gamma_{\text{surf}}^{\text{vdW}}}L_i + 3.60(\text{HA}_{\text{surf}})A_i + 5.11(\text{HD}_{\text{surf}})B_i - 8.47 \quad (11\text{-}12)$$

Using Eq. 11-12, one can quickly see that an apolar compound ($A_i = B_i = 0$) exhibiting an L_i value of about 10 (e.g., PCB 153) will adsorb more than 10 orders of magnitude more strongly from air to graphite than to Teflon.

To apply Eq. 11-12 at different RH, one must simply insert the corresponding surface parameters give in Table 11.1. For example, for the *quartz* surface (qsurf) at RH = 45% and 90%, Eq. 11-12 yields:

$$\log K_{i\text{qsurfa}}(288\text{K}, \text{RH} = 45\%)(\text{m}) = 0.92L_i + 3.20A_i + 5.42B_i - 8.47 \quad (11\text{-}13)$$

and

$$\log K_{i\text{qsurfa}}(288\text{K}, \text{RH} = 90\%)(\text{m}) = 0.72L_i + 3.17A_i + 4.34B_i - 8.47 \quad (11\text{-}14)$$

A comparison of Eqs. 11-13 and 11-14 shows that for the quartz surface, the main effect of RH is on the vdW interaction term, and to a somewhat lesser extent on the H-donating term, since B_i usually has values < 1. The H-accepting properties of the quartz surface show, however, almost no effect with change in RH. As an example of the use of these equations, one finds the $K_{i\text{qsurfa}}$ value of an apolar compound exhibiting an L_i value of about 3 (e.g., tetrachloroethene, PCE) is about 4 times larger at 45% RH than at 90% RH, while for a compound with L_i of about 10 (e.g., PCB 153) the difference is a factor of 100.

Figure 11.7 shows $\log K_{i\text{qsurfa}}$ values predicted with Eq. 11-14 versus experimental data; the pp-LFER equation fits the data quite well. We should point out, however, that Eq. 11-12 has been derived using primarily rather simple, monofunctional compounds covering a rather narrow range in $\log K_{i\text{qsurfa}}$ (−3 to −6 m). For such compounds, predictions within a factor of 2 to 3 are possible (Goss and Schwarzenbach, 2002). However, when applying Eq. 11-12 to more complex, multifunctional compounds, even larger deviations must be expected. Also, application of Eq. 11-12 to compounds exhibiting weak vdW properties, such as the polyfluorinated compounds (HFCs) and the siloxanes, is not optimal as the L_i value does not adequately describe the vdW interactions with surfaces. The reason is that L_i depends, not only on vdW interactions, but also the size of the cavity that has to be formed in hexadecane (see Chapter 7). For almost all other organic compounds, both vdW interactions and cavity formation energy in hexadecane exhibit a similar proportionality to the molecular volume, which is not the case for the HFCs and the siloxanes. Whereas this non-proportionality of the HFCs and the siloxanes cancels out when considering bulk phase partitioning, for adsorption to surfaces, equations using the molar refraction of the compound (i.e., a measure of its polarizability) yield significantly better results (Arp et al., 2006b).

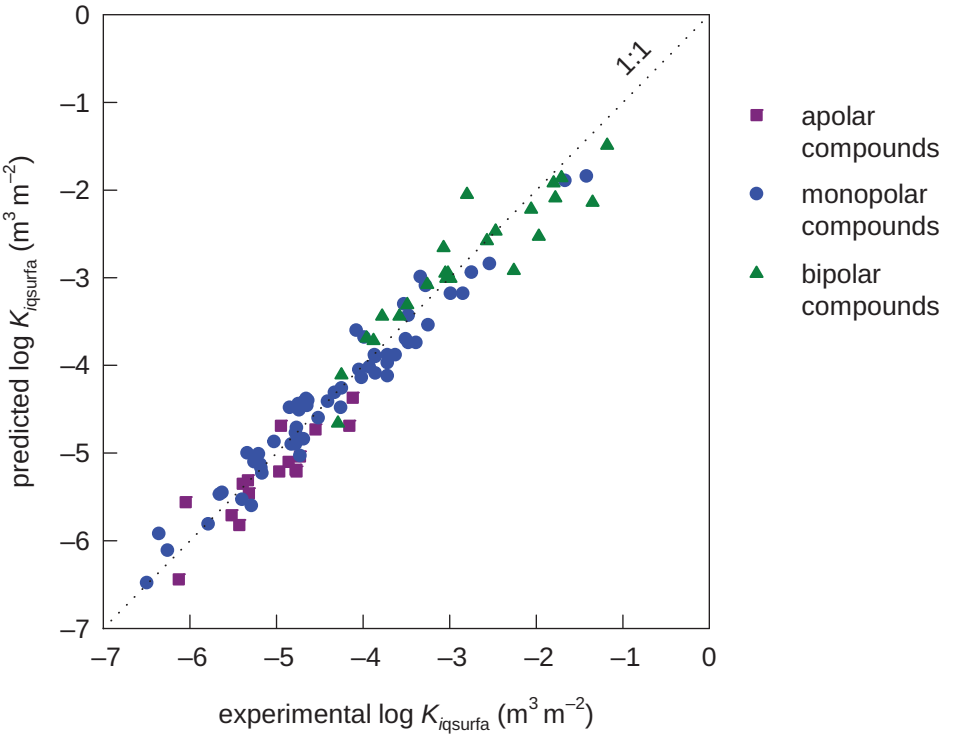

Figure 11.7 Calculated (Eq. 11-14) log$K_{iqsurfa}$ (288K, RH = 90%)(m) versus experimental values for a set of 103 apolar, monopolar, and bipolar compounds. Data from Arp et al. (2006a).

In conclusion, as is illustrated by two examples in Box 11.1, the pp-LFER model Eq. 11-12 using the surface parameters given in Table 11.1 enables us to make calculations concerning the partitioning of organic pollutants between air and well-defined surfaces. However, we should point out that various difficulties exist when applying this model to real-world problems. For example, when we encounter the partitioning of organic compounds between air and aerosols or soils (see Chapter 15), we need to know the types and, particularly, the areas of the dominating (accessible) surfaces present in a given system. To date, experimental data are often reported on a per mass, and not on a per surface area basis, because surface areas are not very well known. Furthermore, surface areas and surface properties may change significantly with changing conditions (e.g., with changing humidity). In addition, the overall partitioning process may be strongly dominated by absorption of a compound into a bulk phase (e.g., water, natural organic material), so that adsorption to a surface is not important anymore (see Chapter 15).

Box 11.1 Estimating the Fraction of Phenanthrene in the Gas Phase and Sorbed to the Walls of a Vessel

Consider two closed air-sampling vessels made out of Teflon and glass (quartz) with an air volume $V_a = 10^{-3}$ m^3 (1 L) and an inner surface area of $A_{surf} = 6{\times}10^{-2}$ m^2 (600 cm^2). In these vessels, you capture air samples that you want to analyze for phenanthrene, which is present at low concentrations. Calculate the fraction of the total phenanthrene present in the air in the two vessels after adsorption equilibrium between the gas phase and the walls of the vessel, which has been established at 15°C (288 K) and 50% relative humidity. Assume that only adsorption at the surface of the walls is important and that the surface is not saturated with phenanthrene. (In reality, absorption could also be important for Teflon, and actually is if one is using "soft" Teflon.)

Teflon is an apolar sorbent that undergoes only vdW interactions. Insert the vdW_{surf} parameter of Teflon (4.2, independent of RH, see Table 11.1) into Eq. 11-12 to obtain:

$$\log K_{i\text{teflona}}(288\text{K})/\text{m} = 0.135(4.4)(7.58) - 8.47 = -3.97$$

or:

$$K_{i\text{teflona}}(288\text{K}) = 1.2 \times 10^{-4}\ \text{m}$$

The fraction of phenanthrene present at equilibrium in the gas phase (air) is given by:

$$f_{i\text{a}} = \frac{C_{i\text{a}}V_\text{a}}{C_{i\text{a}}V_\text{a} + C_{i\text{teflon}}A_\text{teflon}} = \frac{1}{1 + \dfrac{C_{i\text{teflon}}}{C_{i\text{a}}}\dfrac{A_\text{teflon}}{V_\text{a}}} = \frac{1}{1 + K_{i\text{teflona}}\dfrac{A_\text{teflon}}{V_\text{a}}}$$

where $C_{i\text{teflon}}$ is the concentration of phenanthrene per unit surface area. Insert the values of A_teflon and V_a, together with the estimated $K_{i\text{teflona}}$ value into the previous equation to get:

$$f_{i\text{a}} = \frac{1}{1 + (0.00012\ \text{m})(60\ \text{m}^{-1})} = 0.993$$

Thus, virtually all phenanthrene is still present in the gas phase.

Quartz, on the other hand, is a bipolar sorbent that exhibits quite strong H-donor and H-acceptor properties. Phenanthrene is monopolar with $A_i = 0.0$ and $B_i = 0.24$ (see Appendix C). Interpolating linearly, the vdW_{surf} and HD_{surf} values given in Table 11.1 can be found for quartz to obtain the appropriate values for 50% RH:

$$vdW_{quartz}(50\%) = 6.8 - (5/45)(1.5) = 6.6$$
$$HD_{quartz}(50\%) = 1.06 - (5/45)(0.21) = 1.04$$

Inserting these values, together with the phenanthrene's parameters, into Eq. 11-12 yields:

$$\log K_{i\text{qsurfa}}(288\text{K})/\text{m} = 0.135(6.6)(7.58) + 5.11(1.04)(0.24) - 8.47 = -0.44$$

or

$$K_{i\text{qsurfa}}\ (288\text{K}) = 0.36\,\text{m}$$

The fraction of phenanthrene in the air is in this case:

$$f_{i\text{a}} = \frac{1}{1 + (0.36\ \text{m})(60\ \text{m}^{-1})} = 0.04$$

which means that in the glass vessel, 96% of the compound would be lost to the quartz surface.

11.3 Adsorption from Water to Inorganic Surfaces

Although sorption from water to organic matter is commonly dominating the overall sorption of organic compounds in aquatic environments (see Chapter 13), adsorption to inorganic surfaces may prove to be significant under certain conditions. One example is when aquifer solids are derived from sand and gravel beach deposits and contain small organic contents (Schwarzenbach and Westall, 1981; Banerjee et al., 1985; Piwoni and Banerjee, 1989; Ball and Roberts, 1991; Hundal et al., 2001). Additionally, engineered systems such as clay liners are often used to isolate organic wastes buried below ground. While we may be interested in the impact of these low-permeability materials on the subsurface hydraulics, we also need to consider the possibility that those aluminosilicates sorb nonionic organic pollutants and inhibit offsite transport (Boyd et al., 1988). Also, sorption to certain mineral surfaces, even if it is insignificant from a mass balance point of view, may be critical to quantify when dealing with surface-catalyzed transformations (Ulrich and Stone, 1989; Burris et al, 1995). Finally, laboratory glass surfaces may sorb nonionic compounds from aqueous solutions (e.g., Qian et al., 2011), hampering experimental data interpretation.

Nonspecific Adsorption of Nonionic Organic Compounds to Mineral Surfaces

Experimental Findings. Numerous investigators have observed adsorption of apolar and weakly monopolar organic compounds in water to water-wet inorganic surfaces. Generally, adsorption from water to mineral surfaces can be reasonably well described by a concentration-independent partitioning (adsorption) constant, as reported for adsorption of chlorinated compounds like lindane and trichlorobenzene on silica or PAHs on quartz and goethite-covered quartz (Su et al., 2006; Muller et al., 2007). Hence, as for surface–air partitioning, we may define a surface-normalized solid–water adsorption coefficient, $K_{i\mathrm{surfw}}$:

$$K_{i\mathrm{surfw}}(\mathrm{e.g., m}) = \frac{C_{i\mathrm{surf}}(\mathrm{e.g., mol\ m^{-2}})}{C_{iw}(\mathrm{e.g., mol\ m^{-3}})} \tag{11-15}$$

If we chose length (in m) as the dimension, we have actually divided a solid surface area by a volume of water. If the surface area is not known, we may also define a solid–water partition coefficient based on mass, $K_{i\mathrm{sw}}$:

$$K_{i\mathrm{sw}}(\mathrm{e.g., L_w\ kg_s^{-1}}) = \frac{C_{is}(\mathrm{e.g., mol\ kg_s^{-1}})}{C_{iw}(\mathrm{e.g., mol\ L_w^{-1}})} \tag{11-16}$$

We should point out that, particularly when considering highly porous materials exhibiting surface areas of 500 $m^2\ g^{-1}$ and more, the amount of this surface area actually available for adsorption of organic compounds is often unclear (Schwarzenbach and Westall, 1981; Su et al., 2006). Also, nanopores (< 50 nm, see Chapter 5) may play a particularly important role in the adsorption (see Cheng et al., 2012). Therefore, the significant differences observed for surface normalized partition constants of a given compound to the same type of mineral oxide may be, at least partly, due

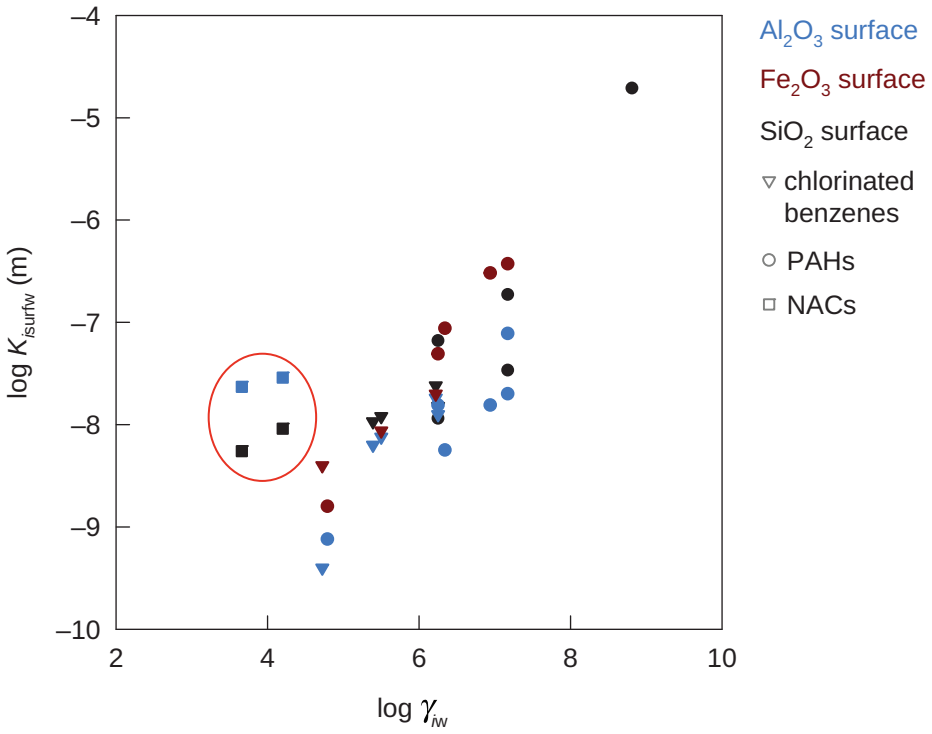

Figure 11.8 Adsorption of chlorinated benzenes, PAHs and NACs (highlighted with red circle) to various mineral oxide surfaces; surface-normalized adsorption constants as a function of the aqueous activity coefficient of the solutes derived from their liquid aqueous solubilities (see Chapter 9; Eqs. 9-5 and 9-8). Data from Schwarzenbach and Westall (1981); Mader et al. (1997); Su et al. (2006); and Muller et al. (2007).

to an erroneous assumption of the actual surface area available for adsorption, leading to a smaller apparent $K_{i\text{surfw}}$ value. Conversely, traces of strongly sorbing organic materials on minerals may lead to a higher apparent adsorption constant.

The absolute values of sorption enthalpies are small (between −15 and −25 kJ mol^{-1}; e.g., Mader et al., 1997; Su et al., 2006). We recall that the excess enthalpies of solution of PAHs and chlorinated benzenes in water are positive, but they exhibit very similar absolute values (Table 9.2). Since we may reasonably anticipate that some of this energy yield of mineral sorption came from the removal of those chemicals from aqueous solution, after accounting for enthalpies of solution, the remaining steps in mineral binding of nonpolar sorbates comes out to be energetically neutral or even slightly endothermic.

Increasing the temperature generally results in diminished adsorption of neutral apolar and weakly monopolar compounds to mineral oxide surfaces; the dependence, however, is rather weak, corresponding with the small values of sorption enthalpy. Also, pH and ionic strength do not significantly affect adsorption (Mader et al., 1997; Su et al., 2006). Further, the presence of competing neutral sorbates does not affect mineral surface adsorption, implying that the sorbates do not compete for specific sorption sites (e.g., Boucher and Lee, 1972; Mader et al., 1997; Su et al., 2006).

From Fig. 11.8, one sees that for adsorption of a given class of compounds (e.g., chlorinated benzenes, PAHs) to a particular mineral surface, the area-normalized sorption coefficient (e.g., log $K_{i\text{surfw}}$ in units of m) tends to correlate quite well with the sorbate's aqueous activity coefficient. Indeed, the higher the log γ_{iw} (the sorbate's

"dislike" of water), the greater the affinity of the compound for the mineral surface. We also note that the dependence of log $K_{i\text{surfw}}$ on γ_{iw} is somewhat more pronounced for the PAHs as compared to the chlorinated benzenes. Finally, we should point out that the nitroaromatic compounds adsorb significantly more strongly than would be expected from their aqueous activity coefficients, suggesting the increased polarity of these nitro- substituted substances may enable favorable near-surface interactions which, in addition to their desire to escape aqueous solution, enhance their adsorption.

Mechanistic Considerations. All the aforementioned experimental observations suggest that significant *specific interactions* between the sorbate molecules and the mineral surface do not drive adsorption. As previously discussed for surface–air partitioning, actual *adsorption* of nonionic organic compounds directly on water-wet hydrophilic inorganic surfaces would require that these organic sorbates displace water molecules already adhering to the polar surface. However, water has much stronger interaction energies on mineral surfaces *per unit area* than apolar and monopolar compounds (see Fig. 11.3), so surface *ad*sorption from bulk water onto fully water-wet hydrophilic solids probably does not explain the sorption of apolar and monopolar organic compounds on minerals.

Instead, the observations suggest the process simply involves partitioning of the neutral sorbates between the bulk water and the "special" water immediately adjacent to solid surfaces and inside the nanometer-sized pores of these solids. Water molecules near inorganic surfaces are more organized than corresponding molecules located in the bulk solution because of their interactions with the solid. Such "special" surface-ordered water films are called *vicinal water* (Fig. 11.9*b*). Being located in this layer of vicinal water may be energetically more favorable for the sorbate. The volume of this vicinal water per mass of sorbent is related to the mineral particle's porosity and surface area. Consequently, the amount of such special near-surface water per mass of solid is greater for fine, porous silica (~ 0.5 mL g^{-1}) than for quartzite sand (< 0.001 mL g^{-1}), and greater for expandable montmorillonite (~ 0.5 mL g^{-1}) than for the two-layer clay, kaolinite (<0.02 mL g^{-1}). Such volumes may approach a milliliter per gram in highly porous solids (Ogram et al., 1985; Mikhail et al., 1968a, b).

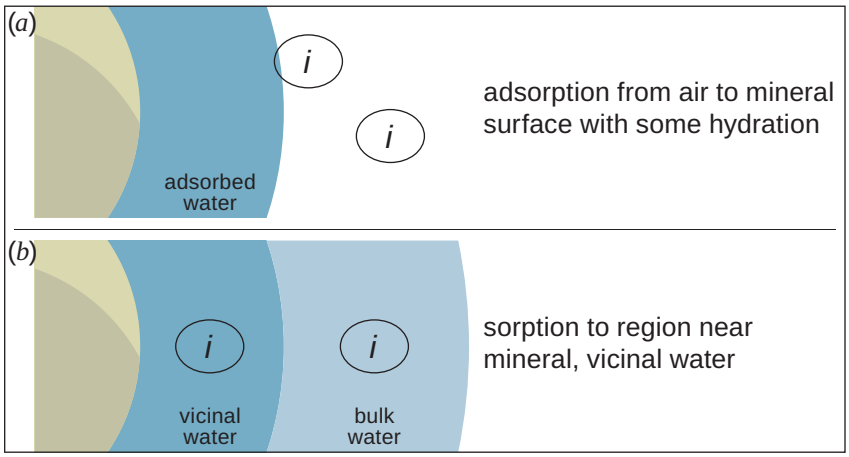

Figure 11.9 Visualization of the difference of how non-specifically interacting organic compounds may sorb to inorganic surfaces from (*a*) air to surfaces with limited water presence (see also Fig. 11.6), and (*b*) partitioning from aqueous solution to the layer of "vicinal water" adjacent to surfaces that serves as an absorbent liquid.

Using this concept of vicinal water, sorption of apolar and monopolar compounds to inorganic solids may best be viewed as partitioning between relatively disorganized bulk water and this special volume of ordered water near the solid's surface:

$$(i)_{\text{bulk water}} + n(H_2O)_{\text{vicinal}} \rightleftharpoons (i)_{\text{vicinal water}} + n(H_2O)_{\text{bulk}} \qquad (11\text{-}17)$$

Such a conceptualization requires a corresponding "desorption" of some number, n, of water molecules from the vicinal region to make a cavity near the solid surface in which i fits.

In general, nonionic compounds of low polarity exhibit only a weak tendency to partition from bulk aqueous solution into the region near mineral surfaces. As the corresponding partitioning mechanism is still uncertain, we do not yet know how to predict such sorption. If empirical results are available from structurally related compounds, parameters such as the aqueous activity coefficient may help us predict the intensity of surface associations for new compounds in the same compound classes (i.e., interpolating data such as that shown in Fig. 11.8). Finally, we should point out that, in the case of adsorption from water to inorganic surfaces, the application of the thermodynamic cycle to calculate $K_{i\text{surfw}}$ from surface–air and air–water partition constants is not possible because the transfer from air to the surface and from air to the surface immersed in water are two completely different processes (see Fig. 11.9*a* and *b*).

Specific Adsorption of Nonionic Organic Compounds to Mineral Surfaces

Experimental Findings. As is illustrated by Fig. 11.8, some nonionic organic compounds (i.e., NACs) exhibit much stronger mineral surface affinities than we see for apolar and weakly monopolar compounds of comparable log γ_{iw}, like chlorobenzenes and PAHs. In these cases, the organic sorbates are able to displace water from the mineral surface and participate in fairly strong sorbate:sorbent intermolecular interactions. One prominent example is the adsorption of nitroaromatic compounds (NACs) to the siloxane surfaces of clay minerals. NACs (e.g., our companion, the explosive 2,4,6-trinitrotoluene (TNT, see margin)) are aromatic compounds that, while overall nonionic, tend to have very uneven electron distributions.

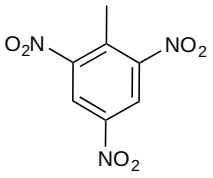

2,4,6-trinitrotoluene (TNT)

NACs exhibit linear isotherms upon adsorption to clays at very low concentrations, but the shape of the isotherm becomes hyperbolic (i.e., fits a so-called Langmuir equation, see Chapter 12; Eq. 12.1) when higher sorbate concentrations are considered (Haderlein and Schwarzenbach, 1993; Haderlein et al., 1996). This saturation behavior indicates a specific sorptive association with a finite number of sorption sites on the solid surface. Observations of competitive effects among different NACs in sorption experiments also indicate specific site interactions affect adsorption. Furthermore, the sorption enthalpies have been found to be much greater than the negative values of the excess enthalpies of aqueous solution of these sorbates (up to -40 kJ mol^{-1}) (Haderlein and Schwarzenbach, 1993; Li et al., 2004).

A particularly distinguishing feature of this type of sorption is that the cation serving as the counterion on charged sites on the minerals affects the intensity of this type of

sorption (Haderlein and Schwarzenbach, 1993; Qu et al., 2011). For example, NAC adsorption to aluminosilicate clays is much greater when potassium or cesium serve as the counterion, balancing the solid's surface charge (see Chapter 14 on ion exchange), rather than calcium or sodium (Haderlein et al., 1996).

Mechanistic Considerations. These various experimental findings make sense when we imagine that NACs can form an *e*lectron *d*onor-*a*cceptor (EDA) complex with the siloxane oxygen molecules on the surface of clay minerals. NACs have an uneven electron distribution in that the strong electron withdrawing nitro groups lower the electron density in the aromatic ring, with concurrent increase in the electron density at the oxygens of the nitro group (see Chapter 4, Section 4.4). This electron deficiency in the aromatic ring becomes stronger the more electron-withdrawing groups (i.e., nitro groups or other electron-withdrawing substituents such as –C≡N, Weissmahr et al., 1999) are attached to the same ring. The electron-depleted region of the ring of a NAC can, therefore, be considered as electron acceptor (δ^+) and the oxygens of the nitro group as electon donors (δ^-).

Figure 11.10 provides a schematic picture of the current hypothesis of the interactions that exists between a given NAC and a siloxane surface of a clay mineral. The siloxane oxygen molecules on a mineral surface can be electron-rich due to isomorphic substitutions in the mineral lattice (see δ^- on siloxane near Al^{3+} in place of Si^{4+}); one can then readily envision the electron-depleted π-clouds of these aromatic compounds accepting electron density from such siloxane oxygen molecules (Fig. 11.10). Large hydrated ions like sodium and calcium may, however, block NAC access to electron rich siloxane sites, while smaller hydrated potassium ions do not (Weissmahr

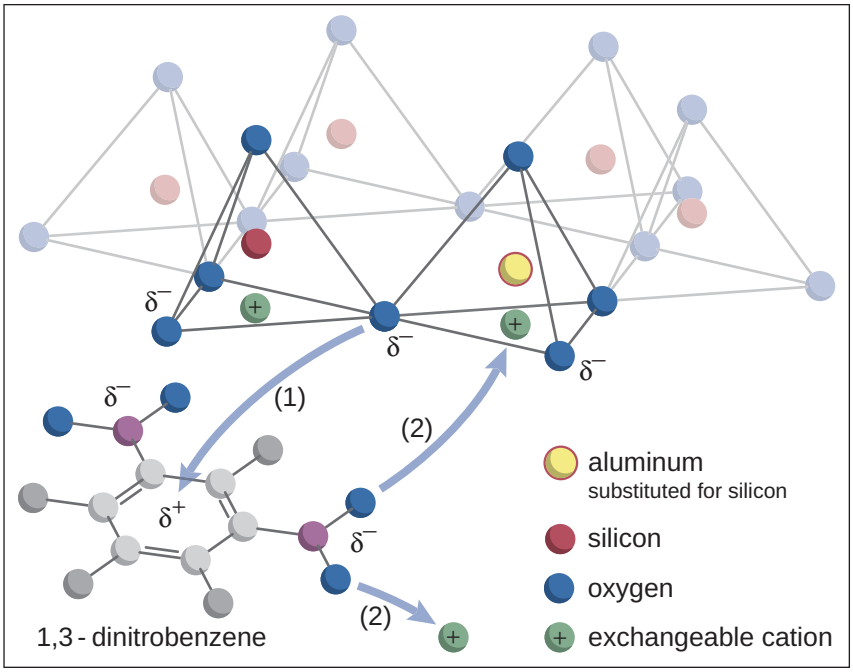

Figure 11.10 Conceptualization of the adsorption of the NAC 1,3-dinitrobenzene to a siloxane surface due to EDA interactions, i.e., (1) attraction of electron-rich siloxane oxygens to the electron depleted "π-cloud" of the aromatic ring, and (2) attraction of the electron-rich oxygens of the nitro groups to the (hydrated) cations serving as counterions. Adapted from Qu et al. (2011).

et al., 1997). Also, the electron-rich oxygens of nitro groups (δ^-) may be attracted to hydrated potassium ions held in place as positively charged counterions to the charged surface (Fig. 11.10). In these scenarios, a very specific directional interaction occurs, in which one partner donates electrons and the other accepts them to form an EDA complex.

We can portray the adsorption process depicted in Fig. 11.11 as:

$$(\mathrm{Si, Al}) > \mathrm{O^-}\colon \mathrm{K^+} \; + \; {}^{\delta+}\mathrm{NAC}^{\delta-} \rightleftharpoons (\mathrm{Si, Al}) > \mathrm{O} :{}^{\delta+}\mathrm{NAC}^{\delta-}\colon \mathrm{K^+} \qquad (11\text{-}18)$$

where the surface species involves electron delivery to the NAC from the siloxane oxygen and/or from the NAC to adsorbed cations like potassium (Eq. 11-18) or ammonium or cesium (Weissmahr et al., 1997). With this exchange in mind and assuming that we are in the linear part of the isotherm, we may define a thermodynamic equilibrium constant:

$$K_{\mathrm{NAC,EDA}}(\mathrm{L\ mol^{-1}sites}) = \frac{[(\mathrm{Si, Al}) > \mathrm{O^-}\colon \mathrm{NAC} : \mathrm{K^+}]}{[\,(\mathrm{Si, Al}) > \mathrm{O^-}\colon \mathrm{K^+}][\mathrm{NAC}]} \qquad (11\text{-}19)$$

where this sorption coefficient has the subscript EDA to remind us that it reflects electron donor-acceptor surface interactions; it has the units that result from the ratio: (mol NAC $\mathrm{kg^{-1}}$ solid) (mol sites $\mathrm{kg^{-1}}$ solid)$^{-1}$ (mol NAC $\mathrm{L^{-1}}$)$^{-1}$ = L $\mathrm{mol^{-1}}$ sites.

Values of $K_{\mathrm{NAC,EDA}}$ have been measured for a large number of NACs and other aromatic derivatives (Table 11.2; Haderlein and Schwarzenbach, 1993; Haderlein et al., 1996). Generally, the values increase as more electron-withdrawing nitro substituents occur on a sorbate (e.g., compare 4-nitrotoluene at 820 versus 2,4-dinitrotoluene at 120,000 versus 2,4,6-trinitrotoluene at 300,000 L $\mathrm{mol^{-1}}$ sites). Also, ring substituents that prevent close approach of the ring system to the siloxane face (e.g., the *sec*-butyl in Dinoseb) lower the value of the $K_{\mathrm{NAC,EDA}}$ significantly (compare Dinoseb with DNOC).

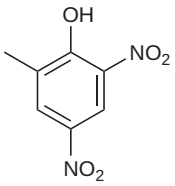

2,4-dinitro-6-methylphenol
(DNOC)

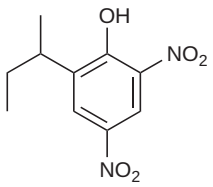

2,4-dinitro-6-sec-butylphenol
(Dinoseb)

The extent of complexation with any particular clay mineral also depends on the abundance of siloxane sites per mass of clay. This surface area factor is defined as 1 for a two-layer clay like kaolinite, is higher for a three-layer clay like illite (about 6 times more than kaolinite), and is greatest for an expandable clay like montmorillonite (about 12 times more than kaolinite). The $K_{\mathrm{NAC,EDA}}$ values provided in Table 11.2 are normalized to the kaolinite case, but these values have to be increased by the appropriate factors to handle sorption to aluminosilicate clays like illite and montmorillonite.

Recognizing that any given clay has a finite number of sites per unit surface area, we can assume the sites are partially filled with NACs and partially filled with competitors, e.g., hydrated $\mathrm{K^+}$:

$$[\text{total sites}] = [(\mathrm{Si, Al}) > \mathrm{O^-}\colon \mathrm{NAC} : \mathrm{K^+(H_2O)_m}] + [(\mathrm{Si, Al}) > \mathrm{O^-}\colon \mathrm{K^+(H_2O)_n}] \qquad (11\text{-}20)$$

Table 11.2 Adsorption of Nonionic Nitroaromatic Compounds (NACs) to Aluminosilicate Clays: (*a*) Surface Area Factors, f_{saf}, for Different Clays Expressing Maximum Sorption Sites Relative to Kaolinite, and (*b*) $K_{NAC,EDA}$ Values (L mol^{-1} sites) Measured for Several NACs on K$^+$-Kaolinite

(*a*) Aluminosilicate Clay	Surface Area Factor (f_{saf})
Kaolinite	1
Illite	6
Montmorillonite	12

(*b*) Compound	K_{NAC}, EDA (L mol^{-1} sites)[a]
Nitrobenzene	100
1,2-Dinitrobenzene	70
1,4-Dinitrobenzene	31,000
2-Nitrotoluene	50
3-Nitrotoluene	420
4-Nitrotoluene	820
2,4-Dinitrotoluene	120,000
2,6-Dinitrotoluene	1,700
2,4,6-Trinitrotoluene (TNT)	300,000
2-Amine-4,6-dinitrotoluene	50,000
4-Amino-2,6-dinitrotoluene	1,800
2,6-Diamino-4-nitrotoluene	180
2,4-Dinitro-6-methyl-phenol (DNOC)	450,000
2,4-Dinitro-6-sec-butyl-phenol (Dinoseb)	1,100

[a]Data from Haderlein et al. (1996)

where the subscripts, *m* and *n* on the water reflect changed degrees of cation hydration when an NAC is present. Now we can substitute for the NAC-free site term in Eq. 11-20, and after rearranging find:

$$[(\mathrm{Si, Al}) > \mathrm{O{:}NAC{:}K^+(H_2O)_m}] = \frac{[\text{total sites}]K_{NAC,EDA}[\mathrm{NAC}]}{1+K_{NAC,EDA}[\mathrm{NAC}]} \qquad (11\text{-}21)$$

or

$$K_{NACclayw} = \frac{[(\mathrm{Si, Al}) > \mathrm{O{:}NAC{:}K^+(H_2O)_m}]}{[\mathrm{NAC}]} = \frac{[\text{total sites}]K_{NAC,EDA}}{1+K_{NAC,EDA}[\mathrm{NAC}]} \qquad (11\text{-}22)$$

In most aquatic systems where Na^+, K^+, Mg^{2+}, and Ca^{2+} serve as the predominant cations, it is only the fraction of the siloxane surface covered by potassium counterions that proves to be accessible to NACs. Therefore, for natural solids in a real world

soil or sediment, the total available sites for such EDA interactions can be approximated by the product:

$$[\text{total sites}] = f_{\text{clay}} \times f_{\text{K+clay}} \times f_{\text{saf}} \times (6\times10^{-3} \text{ mol sites kg}^{-1} \text{ K}^{+}\text{-kaolinite}) \quad (11\text{-}23)$$

where f_{clay} is the clay mineral (not clay size) content of the solids (kg clay kg^{-1} solid), $f_{\text{K+clay}}$ is the fraction of cationic counterion charges contributed by weakly hydrated cations like potassium (kg K^{+}clay kg^{-1} clay), f_{saf} is the average surface area factor reflecting the ratio of siloxane surface availability of the clay minerals present versus kaolinite, and 6×10^{-3} mol sites kg^{-1} K^{+}-kaolinite is the typical value for the maximum site density on kaolinite.

Finally, combining the expression for the total sites with Eq. 11-22, we have:

$$K_{\text{NACclayw}}(\text{L kg}^{-1} \text{ solid}) = \frac{f_{\text{clay}} \cdot f_{\text{K+clay}} \cdot f_{\text{saf}} \ (6\times10^{-3}) K_{\text{NAC,EDA}}}{1 + K_{\text{NAC,EDA}}[\text{NAC}]} \quad (11\text{-}24)$$

For the sake of simplicity, we assume that $f_{\text{K+clay}}$ and $K_{\text{NAC,EDA}}$ are linearly related, which is not necessarily the case (see Weissmahr et al., 1999). Equation 11-24 indicates that K_{NACclayw} is constant at low concentrations (i.e., $[\text{NAC}] \ll 1/K_{\text{NAC,EDA}}$) and declines at higher levels. Now, one may apply knowledge of the clay mineralogy of natural solids and the cationic composition of the aqueous solutions in which they are bathed to estimate the sorption of NACs. Often, this sorption mechanism is even more important than absorption to NOM for NACs with fairly large $K_{\text{NAC,EDA}}$ values (Weissmahr et al., 1999). Finally, we should note that when present in mixtures, competition for sites between different NACs may strongly influence the transport of these contaminants (Haderlein and Schwarzenbach, 1993; Fesch et al., 1998).

11.4 Questions and Problems

Special note: Problem solutions are available on the book's website. Solutions to problems marked with an asterisk are available for everyone. Unmarked problems have solutions only available to teachers, practitioners, and others with special permission.

Questions

Q 11.1

Give examples of environmentally relevant situations in which adsorption of organic vapors on inorganic surfaces is an important partitioning process.

Q 11.2

What intermolecular interactions and corresponding free energy contributions would you suspect to be important for the following sorbate:medium:sorbent combinations:

(a) tetrachloroethene (PCE) partitioning between air and quartz sand?

(b) atrazine partitioning between air and Teflon?

(c) methyl-t-butyl ether (MTBE) partitioning between air and quartz sand?

(d) perfluoro octylethanol (8:2 FTOH) partitioning between air and quartz sand?

(e) 2,2′,4,4′,5,5′-hexachlorobiphenyl (PCB 153) partitioning between water and quartz sand?

(f) phenanthrene partitioning between water and quartz sand?

(g) phenol partitioning between water and quartz sand?

Q 11.3

Why does the sorption of nonpolar organic vapors to polar inorganic surfaces generally decrease with increasing humidity? What about polar compounds? Why does the relative humidity have a negligible influence on sorption of organic vapors to apolar surfaces?

Q 11.4

Storey et al., (1995) reported $K_{i\text{surfa}}$ values for the adsorption of n-alkanes and PAHs from air to quartz at 25 to 30% RH and 70 to 75% RH, respectively. When plotting $K_{i\text{surfa}}$ versus ln $p^*_{i\text{L}}$ (Eq. 11-12) for the various data sets, the following slopes "a" are obtained:

	n-alkanes	PAHs
a (25-30% RH)	1.04	1.22
a (70-75% RH)	0.96	1.18

Would you have expected to find steeper slopes for the PAHs as compared to the n-alkanes? If yes, why? Why are the slopes at low RH somewhat steeper than the ones corresponding to high relative humidities?

Q 11.5

Consider two apolar compounds exhibiting a factor of ten difference in their hexadecane–air partition constant. What differences do you expect for the two compounds in their (a) Teflon–air, and (b) graphite–air adsorption coefficients?

Q 11.6

Why is adsorption of nonionic organic compounds from water to mineral surfaces generally rather weak? Are there any exceptions? In what cases may even weak adsorption become relevant?

Q 11.7

Explain why the following sorbate pairs exhibit the relative $K_{NAC,EDA}$'s indicated for adsorption from water to a siloxane surface (Table 11.2):

(a) $K_{NAC,EDA}$ (2,4-dinitrotoluene) $\gg K_{NAC,EDA}$ (2-nitrotoluene)

(b) $K_{NAC,EDA}$ (1,4-dinitrobenzene) $\gg K_{NAC,EDA}$ (1,2-dinitrobenzene)

(c) $K_{NAC,EDA}$ (DNOC) $\gg K_{NAC,EDA}$ (Dinoseb)

Problems

P 11.1 *Using the Thermodynamic Cycle to Estimate Solid Surface–Water Partition Constants*

Experimentally determined quartz surface–water partition constants of phenanthrene, $K_{iqsurfw}$, are in the order of 10^{-7} to 10^{-8} m at 25°C (Muller et al., 2007; Su et al., 2006). Assume that the thermodynamic cycle is applicable and calculate $K_{iqsurfw}$ at 25°C using the air–water partition constant of phenanthrene given in Appendix C and the $K_{iqsurfa}$ (288K, 90% RH) value estimated from Eq. 11-14. Comment on the result.

P 11.2 *Assessing the Speciation of Bromomethane and of Atrazine in a Quartz Sand*

Consider a confined volume of pure quartz sand exposed to air (RH = 45%), with a porosity $\phi = 0.5$ (see Box 5.4), a density of 2.65 g cm^{-3} and a surface area A = 1 m^2 g^{-1}. What fraction f_{ia} of (a) the fumigant bromomethane and (b) the herbicide atrazine will be present in the pore air at 15°C and at 35°C assuming a linear adsorption isotherm? Comment on the result.

Hint: Consult Box 11.1. Use Eq. 11.4 for estimation of the adsorption enthalpy of the two compounds.

P 11.3 *Designing a Sorption Treatment to Remove 1,1,2,2-Tetrachloroethane ($CHCl_2$-$CHCl_2$) from a Waste Gas Stream*

A process in your company generates waste gases that need to be vented to the outside at a rate of 1 m^3 per hour. In particular, you must be sure that the 1,1,2,2-tetrachloroethane present at 100 ppmv (i.e., 100×10^{-6} m^3 of 1,1,2,2-tetrachloroethane vapor per m^3 of total gas) must be removed from the gas stream before discharge. A colleague suggests that you construct an adsorbent column filled with alumina (Al_2O_3) and run the gas through that column to capture the 1,1,2,2-tetrachloroethane.

(a) If the waste gas stream is somewhat dry (i.e., 60% RH) and warm (30°C), how many hours of waste gas can you treat with a 10 m^3 tank of alumina (packed bed porosity 0.3, density 4 g mL^{-1}, with a specific surface area of 10 m^2 g^{-1}, and assumed surface properties like those measured for corundum, see Table 11.1). Assume the 1,1,2,2-tetrachloroethane "breaks through" at a volume equal to the tank's void volume (i.e., number of cubic meters in tank that are filled with gas) divided by the venting

gas flow rate and by the equilibrium fraction of 1,1,2,2-tetrachloroethane in the gas phase.

(b) If you could construct a tank with the same void volume and surface area of silica, would it be more effective? What about activated carbon? Explain your reasoning.

Hint: See Box 11.1 for calculating the fraction in the gaseous and adsorbed phase.

P 11.4 *Where do Organic Compounds Sit in a Fog Droplet? Inside or at the Surface?*

Several studies have shown that the concentrations of many organic pollutants in fog water are much higher than would be expected from the compound's equilibrium air/water partition constant $K_{i\mathrm{aw}}$. In order to describe the observed enrichment of compounds in fog water, an enrichment factor EF can be defined (see, e.g., Goss, 1994 and references cited therein):

$$\mathrm{EF} = \frac{K_{i\mathrm{aw}}}{D_{i\mathrm{aw}}}$$

where $D_{i\mathrm{aw}}$ = *total* concentration of *i* in the gas phase/total concentration of *i* in the fog droplet ($D_{i\mathrm{aw}} = C_{i\mathrm{a}}/C_{i\mathrm{wtot}}$). One possible cause for an enrichment (i.e., $D_{i\mathrm{aw}} < K_{i\mathrm{aw}}$) is the presence of colloidal organic material in the fog droplet, with which the organic compounds may associate (see Chapters 13 and 15). Another possibility suggested by several authors (e.g., Perona, 1992; Valsaraj et al., 1993; Goss, 1994) is enrichment by adsorption at the air–water interface, that is, at the surface of the fog droplet. Is this a reasonable assumption for any organic compound? Estimate the enrichment factor due to surface adsorption at equilibrium for a fog droplet (consisting of pure water) of 8 μm diameter with a surface area (A_d) to volume (V_d) ratio, r_sv, of 7500 $\mathrm{cm^2\ cm^{-3}}$ for (a) tetrachloroethene, (b) phenanthrene and (c) benzo(a)pyrene at 15°C. Neglect the fact that the surface is curved.

Hint: Express the total concentration, $C_{i\mathrm{wt}}$, in the fog droplet by $(A_\mathrm{d}C_{i\mathrm{surf}} + V_\mathrm{d}C_{i\mathrm{w}})/V_\mathrm{d}$ where $A_\mathrm{d}/V_\mathrm{d} = r_\mathrm{sv}$ and $C_{i\mathrm{surf}} = C_{i\mathrm{a}}K_{i\mathrm{surfa}}$. $C_{i\mathrm{surf}}$, $C_{i\mathrm{w}}$, and $C_{i\mathrm{a}}$ are the surface concentration, the bulk water concentration, and the bulk air concentration of *i,* respectively. $K_{i\mathrm{surfa}}$ can be estimated by Eq. 11-11.

11.5 Bibliography

Arp, H. P. H.; Goss, K. U.; Schwarzenbach, R. P., Evaluation of a predictive model for air/surface adsorption equilibrium constants and enthalpies. *Environ. Toxicol. Chem.* **2006a**, *25*(1), 45–51.

Arp, H. P. H.; Niederer, C.; Goss, K. U., Predicting the partitioning behavior of various highly fluorinated compounds. *Environ. Sci. Technol.* **2006b**, *40*(23), 7298–7304.

Atkinson, D.; Curthoys, G., The determination of heats of adsorption by gas-solid chromatography. *J. Chem. Educ.* **1978**, *55*(9), 564–566.

Ball, W. P.; Roberts, P. V., Long-term sorption of halogenated organic chemicals by aquifer material. 1. Equilibrium. *Environ. Sci. Technol.* **1991**, *25*(7), 1223–1237.

Banerjee, P.; Piwoni, M. D.; Ebeid, K., Sorption of organic contaminants to a low carbon subsurface core. *Chemosphere* **1985**, *14*(8), 1057–1067.

Bhatnagar, N.; Kamath, G.; Potoff, J. J., Prediction of 1-octanol-water and air-water partition coefficients for nitro-aromatic compounds from molecular dynamics simulations. *Phys. Chem. Chem. Phys.* **2013**, *15*(17), 6467–6474.

Boucher, F. R.; Lee, G. F., Adsorption of lindane and dieldrin pesticides on unconsolidated aquifer sands. *Environ. Sci. Technol.* **1972**, *6*(6), 538–543.

Boyd, S. A.; Mortland, M. M.; Chiou, C. T., Sorption characteristics of organic compounds on hexadecyltrimethylammonium-smectite. *Soil Sci. Soc. Am. J.* **1988**, *52*(3), 652–657.

Burris, D. R.; Campbell, T. J.; Manoranjan, V. S., Sorption of trichloroethylene and tetrachloroethylene in a batch reactive metallic iron-water system. *Environ. Sci. Technol.* **1995**, *29*(11), 2850–2855.

Cheng, H. F.; Hu, E. D.; Hu, Y. A., Impact of mineral micropores on transport and fate of organic contaminants: A review. *J. Contam. Hydrol.* **2012**, *129*, 80–90.

Chiou, C. T.; Shoup, T. D., Soil sorption of organic vapors and effects of humidity on sorptive mechanism and capacity. *Environ. Sci. Technol.* **1985**, *19*(12), 1196–1200.

de Boer, J. H., *The Dynamical Character of Adsorption*. 2nd ed.; Clarendon Press: Oxford, **1968**; p 240.

Fesch, C.; Simon, W.; Haderlein, S. B.; Reichert, P.; Schwarzenbach, R. P., Nonlinear sorption and nonequilibrium solute transport in aggregated porous media: Experiments, process identification and modeling. *J. Contam. Hydrol.* **1998**, *31*(3-4), 373–407.

Fowkes, F. M., Attractive forces at interfaces. *Ind. Eng. Chem.* **1964**, *56*(12), 40–52.

Goss, K. U., Predicting the enrichment of organic compounds in fog caused by adsorption on the water surface. *Atmos. Environ.* **1994**, *28*(21), 3513–3517.

Goss, K. U., Conceptual model for the adsorption of organic compounds from the gas phase to liquid and solid surfaces. *Environ. Sci. Technol.* **1997**, *31*(12), 3600–3605.

Goss, K. U., The air/surface adsorption equilibrium of organic compounds under ambient conditions. *Crit. Rev. Environ. Sci. Technol.* **2004**, *34*(4), 339–389.

Goss, K. U.; Buschmann, J.; Schwarzenbach, R. P., Determination of the surface sorption properties of talc, different salts, and clay minerals at various relative humidities using adsorption data of a diverse set of organic vapors. *Environ. Toxicol. Chem.* **2003**, *22*(11), 2667–2672.

Goss, K. U.; Schwarzenbach, R. P., Quantification of the effect of humidity on the gas/mineral oxide and gas/salt adsorption of organic compounds. *Environ. Sci. Technol.* **1999a**, *33*(22), 4073–4078.

Goss, K. U.; Schwarzenbach, R. P., Empirical prediction of heats of vaporization and heats of adsorption of organic compounds. *Environ. Sci. Technol.* **1999b**, *33*(19), 3390–3393.

Goss, K. U.; Schwarzenbach, R. P., Adsorption of a diverse set of organic vapors on quartz, $CaCO_3$, and alpha-Al_2O_3 at different relative humidities. *J. Colloid Interface Sci.* **2002**, *252*(1), 31–41.

Haderlein, S. B.; Schwarzenbach, R. P., Adsorption of substituted nitrobenzenes and nitrophenols to mineral surfaces. *Environ. Sci. Technol.* **1993**, *27*(2), 316–326.

Haderlein, S. B.; Weissmahr, K. W.; Schwarzenbach, R. P., Specific adsorption of nitroaromatic: explosives and pesticides to clay minerals. *Environ. Sci. Technol.* **1996**, *30*(2), 612–622.

Hundal, L. S.; Thompson, M. L.; Laird, D. A.; Carmo, A. M., Sorption of phenanthrene by reference smectities. *Environ. Sci. Technol.* **2001**, *35*(17), 3456–3461.

Li, H.; Teppen, B. J.; Johnston, C. T.; Boyd, S. A., Thermodynamics of nitroaromatic compound adsorption from water by smectite clay. *Environ. Sci. Technol.* **2004**, *38*(20), 5433–5442.

Mader, B. T.; Goss, K. U.; Eisenreich, S. J., Sorption of nonionic, hydrophobic organic chemicals to mineral surfaces. *Environ. Sci. Technol.* **1997**, *31*(4), 1079–1086.

Mikhail, R. S.; Brunauer, S.; Bodor, E. E., Investigations of a complete pore structure analysis. I. Analysis of micropores. *J. Colloid Interface Sci.* **1968a**, *26*(1), 45–53.

Mikhail, R. S.; Brunauer, S.; Bodor, E. E., Investigations of a complete pore structure analysis. 2. Analysis of four silica gels. *J. Colloid Interface Sci.* **1968b**, *26*(1), 54–61.

Muller, S.; Totsche, K. U.; Kogel-Knabner, I., Sorption of polycyclic aromatic hydrocarbons to mineral surfaces. *Eur. J. Soil Sci.* **2007**, *58*(4), 918–931.

Ogram, A. V.; Jessup, R. E.; Ou, L. T.; Rao, P. S. C., Effects of sorption on biological degradation rates of (2,4-dichlorophenoxy) acetic acid in soils. *Appl. Environ. Microbiol.* **1985**, *49*(3), 582–587.

Perona, M. J., The solubility of hydrophobic compounds in aqueous droplets. *Atmos. Environ. Part A Gen. Topics* **1992**, *26*(14), 2549–2553.

Piwoni, M. D.; Banerjee, P., Sorption of volatile organic solvents from aqueous solution onto subsurface solids. *J. Contam. Hydrol.* **1989**, *4*(2), 163–179.

Qian, Y. A.; Posch, T.; Schmidt, T. C., Sorption of polycyclic aromatic hydrocarbons (PAHs) on glass surfaces. *Chemosphere* **2011**, *82*(6), 859–865.

Qu, X. L.; Zhang, Y. J.; Li, H.; Zheng, S. R.; Zhu, D. Q., Probing the specific sorption sites on montmorillonite using nitroaromatic compounds and hexafluorobenzene. *Environ. Sci. Technol.* **2011**, *45*(6), 2209–2216.

Roth, C. M.; Goss, K. U.; Schwarzenbach, R. P., Adsorption of a diverse set of organic vapors on the bulk water surface. *J. Colloid Interface Sci.* **2002**, *252*(1), 21–30.

Schwarzenbach, R. P.; Westall, J., Transport of nonpolar organic compounds from surface water to groundwater. Laboratory sorption studies. *Environ. Sci. Technol.* **1981**, *15*(11), 1360–1367.

Storey, J. M. E.; Luo, W.; Isabelle, L. M.; Pankow, J. F., Gas/solid partitioning of semivolatile organic compounds to model atmospheric solid surfaces as a function of relative humidity. 1. Clean quartz. *Environ. Sci. Technol.* **1995**, *29*(9), 2420–2428.

Su, Y. H.; Zhu, Y. G.; Sheng, G.; Chiou, C. T., Linear adsorption of nonionic organic compounds from water onto hydrophilic minerals: Silica and alumina. *Environ. Sci. Technol.* **2006**, *40*(22), 6949–6954.

Ulrich, H. J.; Stone, A. T., The oxidation of chlorophenols adsorbed to manganese oxide surfaces. *Environ. Sci. Technol.* **1989**, *23*(4), 421–428.

Valsaraj, K. T.; Thoma, G. J.; Reible, D. D.; Thibodeaux, L. J., On the enrichment of hydrophobic organic compounds in fog droplets. *Atmos. Environ. Part A Gen. Topics* **1993**, *27*(2), 203–210.

Weissmahr, K. W.; Haderlein, S. B.; Schwarzenbach, R. P.; Hany, R.; Nuesch, R., *In situ* spectroscopic investigations of adsorption mechanisms of nitroaromatic compounds at clay minerals. *Environ. Sci. Technol.* **1997**, *31*(1), 240–247.

Weissmahr, K. W.; Hildenbrand, M.; Schwarzenbach, R. P.; Haderlein, S. B., Laboratory and field scale evaluation of geochemical controls on groundwater transport of nitroaromatic ammunition residues. *Environ. Sci. Technol.* **1999**, *33*(15), 2593–2600.